

Article

Oxidative *N*-Formylation of Secondary Amines Catalyzed by Reusable Bimetallic AuPd–Fe₃O₄ Nanoparticles

Sabyuk Yang, Ahra Cho [†], Jin Hee Cho [†] and Byeong Moon Kim * 

Department of Chemistry, College of Natural Sciences, Seoul National University, Seoul 08826, Korea; diablopkk@snu.ac.kr (S.Y.); araelliecho@snu.ac.kr (A.C.); 201722658@snu.ac.kr (J.H.C.)

* Correspondence: kimbm@snu.ac.kr

[†] These authors contributed equally to this work.

Abstract: Bimetallic catalysts are gaining attention due to their characteristics of promoting reactivity and selectivity in catalyzed reactions. Herein, a new catalytic *N*-formylation of secondary amines using AuPd–Fe₃O₄ at room temperature is reported. Methanol was utilized as the formyl source and 1.0 atm of O₂ gas served as an external oxidant. The bimetallic catalyst, consisting of Au and Pd, makes the reaction more efficient than that using each metal separately. In addition, the catalyst can be effectively recycled owing to the Fe₃O₄ support.

Keywords: formylation; gold nanoparticle; heterogeneous catalysis; methanol; bimetallic catalyst; recyclable catalyst



Citation: Yang, S.; Cho, A.; Cho, J.H.; Kim, B.M. Oxidative *N*-Formylation of Secondary Amines Catalyzed by Reusable Bimetallic AuPd–Fe₃O₄ Nanoparticles. *Nanomaterials* **2021**, *11*, 2101. <https://doi.org/10.3390/nano11082101>

Academic Editor: Evgeny Gerasimov

Received: 12 July 2021

Accepted: 16 August 2021

Published: 18 August 2021

Publisher's Note: MDPI stays neutral with regard to jurisdictional claims in published maps and institutional affiliations.



Copyright: © 2021 by the authors. Licensee MDPI, Basel, Switzerland. This article is an open access article distributed under the terms and conditions of the Creative Commons Attribution (CC BY) license (<https://creativecommons.org/licenses/by/4.0/>).

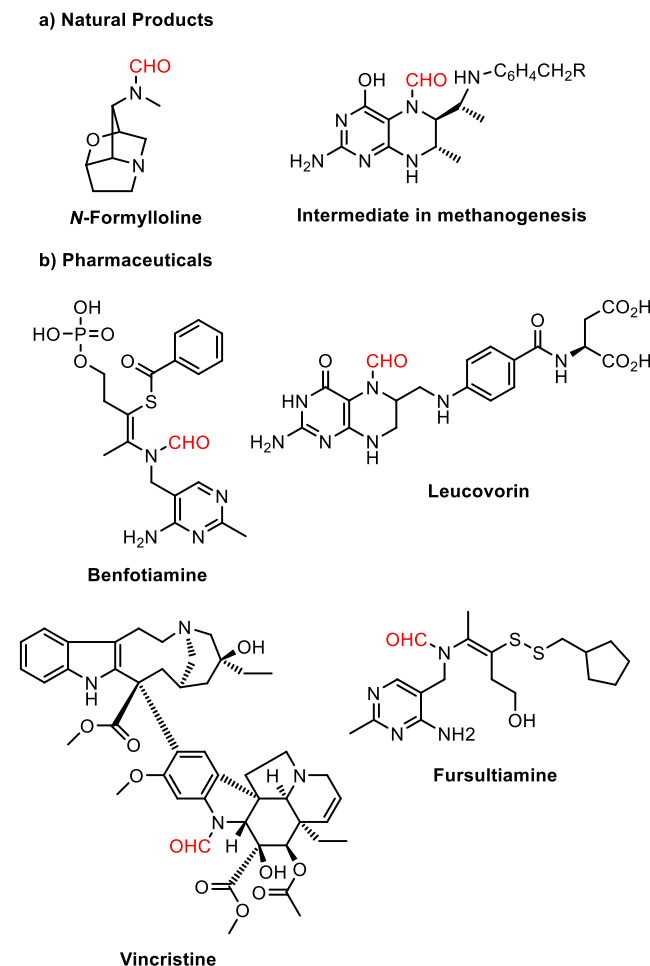
1. Introduction

Formamide groups are important in organic chemistry because of their abundance in natural products or utility as a valuable intermediate in synthesis (Scheme 1a), and pharmaceuticals (Scheme 1b) [1]. For example, this moiety is found in *N*-formyllooline, an alkaloid produced by grass [2], and acts as an intermediate in biochemical processes, such as methanogenesis [3]. Some examples of formamide-containing drugs are benfotiamine (diabetic neuropathy) [4], leucovorin (toxic effects of methotrexate and pyrimethamine) [5], vincristine (anticancer) [6], and fursultiamine (thiamine deficiency) [7]. Considering the prevalence and importance of the formamide functionality, many researchers have developed efficient methods for attaching a formyl group to an amine [8–10]. One of the most direct methods to synthesize formamides is the direct *N*-formylation of amines with a formate ester, organosilicon reagent, formic acid or cyanide [8,9,11–14]. However, this process generates halide byproducts, and more environmentally friendly methods using green formyl sources have been actively pursued [15–17].

Among formyl sources, methanol is an ideal C₁ source because of its availability and ecofriendly properties compared with other reagents [18,19]. It is one of the most popular C₁ sources in organic reactions, such as methylation [20–24], formylation [25–27], and methoxylation [28–30], forming C–C, C–N, and C–O bonds, respectively. Therefore, developing a new catalytic route for the synthesis of formamides with methanol as a sustainable building block would be a valuable addition to the synthetic toolbox.

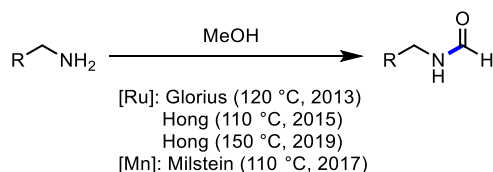
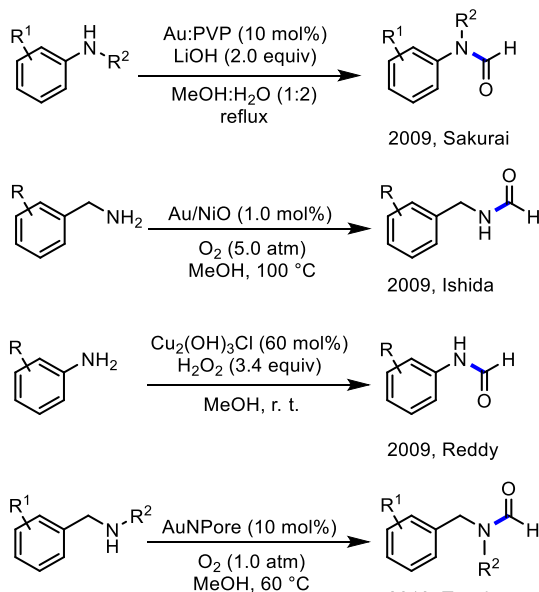
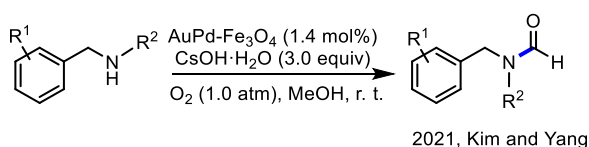
Currently, there are a handful of catalytic *N*-formylation reactions of amines with methanol in the literature (Scheme 2). Both homogeneous and heterogeneous catalysts have been widely used for this transformation. Homogeneous catalysts are one of the most popular tools, owing to their high reactivities (Scheme 2a) [31–33]. For example, Glorius and coworkers reported the *N*-formylation of amines catalyzed by the Ru–NHC catalyst in 2013 [34]. In 2017, the Milstein group achieved the acceptorless dehydrogenative coupling of methanol and amines using a manganese catalyst [35]. Hong and coworkers reported the *N*-formylation of amines with methanol in the presence of ruthenium catalysts in 2015 and 2019 [36,37]. In addition to these representative examples, various transition metal

catalysts have been employed in *N*-formylation [38–44]. However, despite their merits, homogeneous catalysts are generally difficult to recover and show low stability compared to heterogeneous catalysts. Therefore, heterogeneous catalysts have been considered as alternatives because of their recyclability and ease of handling (Scheme 2b) [26,45–47]. Au-containing heterogeneous catalysts have often been employed as highly efficient catalysts for the oxidation of alcohols and their coupling reactions with other reactants [48–51].



Scheme 1. Formamide groups found in natural products and pharmaceuticals: (a) natural products; (b) pharmaceuticals.

For example, in 2009, Sakurai and coworkers reported the *N*-formylation of anilines using Au nanoclusters stabilized by poly(*N*-vinylpyrrolidone) (Au:PVP) [52]. In the same year, Ishida et al. developed the *N*-formylation of benzylamine using supported Au nanoparticles, such as Au/NiO or Au/Al₂O₃ [53]. Using hydrogen peroxide as an oxidant, Reddy developed the room-temperature *N*-formylation of amines using a copper catalyst [54]. In 2013, the reaction of aliphatic amines using AuNPore under 1.0 atm of O₂ gas was developed by Tanaka et al. [55]. However, most of these reactions require high temperatures or high O₂ gas pressures. Therefore, the development of a simple experimental procedure under relatively mild conditions is still required.

a) *N*-Formylation of amines with methanol (Homogeneous)b) *N*-Formylation of amines with methanol (Heterogeneous)c) This work: *N*-Formylation of secondary amines with methanol using bimetallic AuPd-Fe₃O₄ catalyst

- Recyclable bimetallic catalyst
- Mild condition
- High yield

Scheme 2. *N*-Formylation of amines using methanol as a C₁ source: (a) homogeneous catalysis; (b) heterogeneous catalysis; (c) This work.

Based on our continuous efforts toward the development of metal nanoparticle-Fe₃O₄ catalysts, such as Pd-Fe₃O₄ [56], we developed a series of heterogeneous transition metal nanocatalysts for efficient organic transformations [57–62]. In particular, bimetallic combinations of various transition metals on an Fe₃O₄ support have been very useful catalysts for efficient, selective organic transformations [63–67]. Because Au nanoparticle catalysts have been widely used in a variety of oxidative reactions, we prepared bimetallic AuPd-Fe₃O₄ nanoparticle catalysts for selective redox reactions and developed the efficient reductive amination of nitroarenes and aldehydes [65] and oxidative conversion of 5-hydroxymethylfurfural to furan-2,5-dimethylcarboxylate [66].

Herein, we report a new and efficient protocol for secondary amine *N*-formylation through methanol oxidation, using AuPd-Fe₃O₄ as a reusable catalyst (Scheme 2c). Methanol serves not only as the formylating agent, but also as the solvent, and the reaction proceeds at room temperature under 1.0 atm of O₂ gas as an external oxidant.

2. Materials and Methods

All commercially available chemicals were used as received without further purification. $\text{HAuCl}_4 \cdot 3\text{H}_2\text{O}$ (+49% Au basis) and PdCl_2 (99% purity) were purchased from Alfa Aesar (Ward Hill, MA, USA). *N*-methyl-1-phenylmethanamine and polyvinylpyrrolidone (PVP) were purchased from Sigma-Aldrich (St. Louis, MO, USA). Cesium hydroxide monohydrate was purchased from Acros Organics (Pittsburgh, PA, USA). Fe_3O_4 NPs were purchased from DK nano technology (Beijing, China).

3. Results

3.1. Catalyst Characterization

The bimetallic $\text{AuPd-Fe}_3\text{O}_4$ catalyst was synthesized following a procedure previously developed in our laboratories [65]. Adding palladium(II) chloride (PdCl_2) in ethylene glycol, gold(III) chloride trihydrate ($\text{HAuCl}_4 \cdot 3\text{H}_2\text{O}$) in water, and aqueous sodium borohydride solution dropwise sequentially to a Fe_3O_4 solution in water and stirring under 60 °C for 5 h afforded $\text{AuPd-Fe}_3\text{O}_4$ nanoparticles. These were characterized by scanning electron microscopy (SEM, Figure S1) by JSM-7800F Prime (JEOL Ltd., Tokyo, Japan), energy-dispersive X-ray spectroscopy (EDS, Figures S2 and S3) by JSM-7800F Prime (JEOL Ltd., Tokyo, Japan), high-resolution transmission electron microscopy (HR-TEM, Figures S4 and S6) by JEM-3010 (JEOL Ltd., Tokyo, Japan), scanning transmission electron microscopy (STEM, Figure S5) by JEM-ARM200F (JEOL Ltd., Tokyo, Japan), and X-ray photoelectron spectroscopy (XPS, Figure S7) by AXIS SUPRA (Kratos Analytical Ltd., Manchester, UK). The binding energy peaks of Pd 3d in $\text{Pd-Fe}_3\text{O}_4$ were positioned at 339.8 and 334.6 eV, corresponding to Pd(0) species. Au 4f peaks appeared at 86.9 and 83.3 eV for $\text{Au-Fe}_3\text{O}_4$, indicating the presence of Au(0) species. For $\text{AuPd-Fe}_3\text{O}_4$, the Pd 3d peaks appeared at 339.6 and 334.3 eV and the Au 4f peaks appeared at 86.8 and 83.1 eV, slightly lower than those of the corresponding monometallic nanoparticles. This phenomenon appears to stem from the interaction of Pd and Au, changing the electronic structure because of the formation of an AuPd alloy [68–71]. The lowered binding energy of Au(0) is expected to result from the electron transfer from Pd to Au. However, the reason why the Pd(0) peak shifted to a slightly lower value is not fully understood. SEM, HR-TEM, and STEM images show that Au and Pd were successfully deposited as an alloy on the iron oxide support (Figures 1 and 2a and Figure S5), with the Au and Pd atoms randomly distributed. $\text{AuPd-Fe}_3\text{O}_4$ X-ray diffraction (XRD) data obtained by D8 Advance (Bruker, Billerica, MA, USA) compared with those of both $\text{Au-Fe}_3\text{O}_4$ and $\text{Pd-Fe}_3\text{O}_4$ revealed that the $\text{AuPd-Fe}_3\text{O}_4$ is made up with Au–Pd bimetallic alloy dispersed on the Fe_3O_4 surface (Figure 2b and Figure S9). Inductively coupled plasma-atomic emission spectroscopy (ICP-AES) data obtained by OPTIMA 8300 (Perkin-Elmer, Waltham, MA, USA) revealed that the $\text{AuPd-Fe}_3\text{O}_4$ nanoparticles (NPs) consist of 8.92 wt% Au and 5.19 wt% Pd at a molar ratio of 1.00:1.08 (Figure S8).

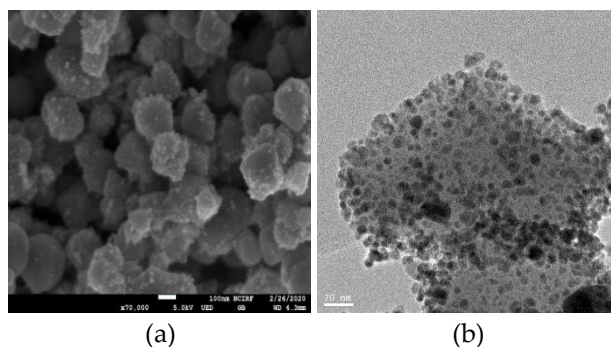


Figure 1. (a) SEM and (b) HR-TEM image of $\text{AuPd-Fe}_3\text{O}_4$ catalyst.

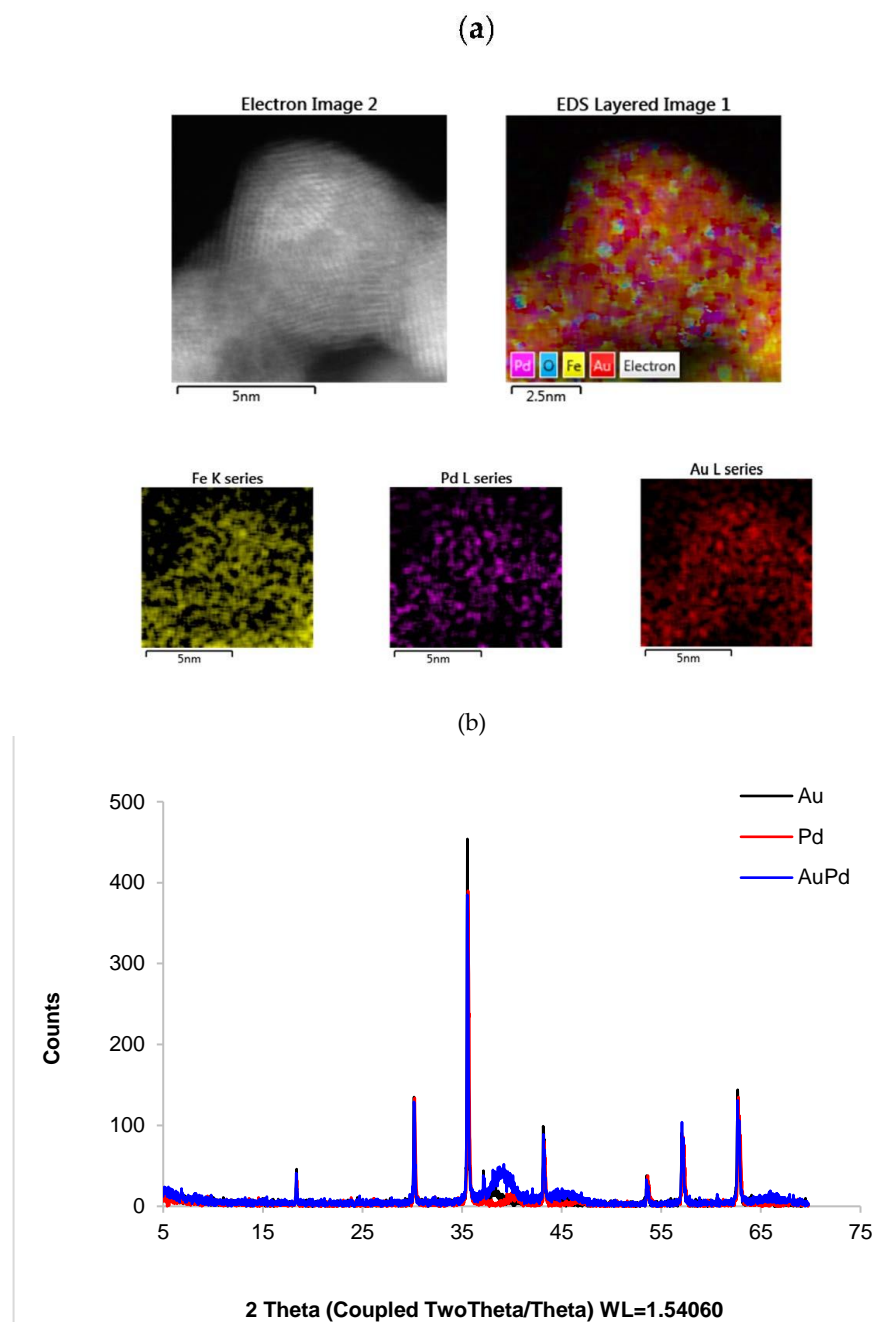


Figure 2. (a) STEM-EDS image and (b) XRD data of AuPd-Fe₃O₄ catalyst.

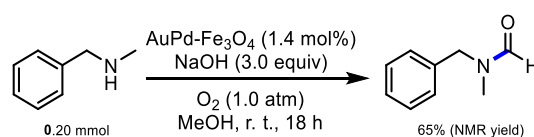
3.2. Reaction Optimization

Following successful preparation of AuPd-Fe₃O₄, we sought the optimum reaction conditions for the *N*-formylation of amines under oxidative conditions. We chose methanol as the formyl group source because it can be readily oxidized to formaldehyde, forming an hemiaminal upon reaction with an amine. We hypothesized that the resulting hemiaminal could be further oxidized to an *N*-formyl group under catalytic oxidation conditions with AuPd-Fe₃O₄ catalyst.

Because the formylation of amine by methanol requires the oxidation of methanol to an hemiaminal and subsequent dehydrogenation of the hemiaminal, an appropriate oxidant should be selected. Various oxidants have been used for alcohol oxidation [72–74]. O₂ gas was chosen as the oxidizing agent to avoid chemical waste problems [75–81].

Initially, a primary amine, such as benzylamine, was mixed with 1.4 mol% of AuPd-Fe₃O₄ (2.8 mol% of total metal contents except for Fe) and methanol under 1.0 atm of O₂

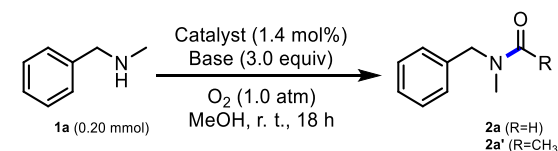
gas, but no *N*-benzylformamide product was detected, while the starting material remained. Subsequently, we added 3.0 equivalents of sodium hydroxide, which led to the formation of *N*-benzylformamide in 25% yield after 18 h. In addition, several unknown high-molecular-weight products, along with a small amount of benzonitrile, were detected from liquid chromatography-mass spectrometry (LC-MS) analysis of the crude mixture. These results suggest that the base plays an important role in the conversion of the amine substrate. According to a report from Mallat group [75], bases are known to facilitate hydrogen abstraction in alcohol dehydrogenation with Au catalysts. However, because the reaction of a primary amine did not yield a clean formylation product, we focused our attention on the formylation of secondary amines. Our first reaction of *N*-methyl-1-phenylmethanamine with methanol, in the presence of AuPd-Fe₃O₄ with sodium hydroxide as a base, yielded the desired *N*-benzyl-*N*-methylformamide in 65% NMR yield (Scheme 3).



Scheme 3. Initial observation of formamide under AuPd-Fe₃O₄.

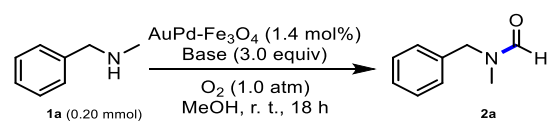
Based on these initial findings, various reaction conditions were tested, and the results are presented in Table 1 and Tables S1–S3. Using *N*-methyl-1-phenylmethanamine (**1a**) as a standard substrate, we tested various reaction conditions with methanol as the formylating agent. Using only iron oxide as a catalyst and sodium hydroxide as a base resulted no progress of the reaction at all (entry 1). However, a reaction with 2.8 mol% Pd-Fe₃O₄ catalyst furnished *N*-benzyl-*N*-methylformamide (**2a**) at a 55% yield (entry 2). Reactions with other monometallic catalysts, such as Au-Fe₃O₄, showed low reactivity (entry 3). The use of the AuPd-Fe₃O₄ bimetallic catalyst afforded the product in 65% yield (entry 4). Without a base, the reaction was sluggish (entry 5). When the O₂ balloon was replaced with an air balloon, the reactivity lowered to afford the desired product at only 43% yield (entry 6). By changing the base to cesium carbonate, we observed a yield similar to that of the reaction using sodium hydroxide (entry 7). However, other inorganic bases were not as effective as hydroxide bases. The reaction using cesium hydroxide monohydrate afforded 90% yield under the same conditions (entry 8). Furthermore, the reaction yield was maintained when the reaction was scaled up to 0.50 mmol (entry 9). The reaction was complete in 4 h when the substrate concentration was increased from 0.20 to 1.0 M, resulting in 89% yield (entry 10). A reaction using ethanol instead of methanol afforded the acetylated product in 42% yield (entry 11). The catalyst loading could be low as 0.40 mol% without significant loss of yield, which is translated to high turnover number (TON) (entry 12 and Table S3).

Knowing that hydroxide bases were effective, we performed further investigations with bases (Table 2 and Table S2). Without a base, only 14% yield of **2a** was obtained (entry 1). Reactions employing LiOH·H₂O and NaOH resulted in 60% and 65% yields, respectively, of the desired products (entries 2 and 3). The use of slightly stronger hydroxide bases, such as KOH or CsOH·H₂O, ensured 75% and 91% yields, respectively (entries 4 and 5). However, carbonate bases were not as effective as hydroxide bases (entries 6 and 7). Reaction yields obtained with other bases, including KO^{*t*}Bu, K₃PO₄, and CsF, were moderate (entries 8–10). In summary, CsOH·H₂O was the optimal base.

Table 1. Screening data of the *N*-formylation of amine ¹.


| Entry | Catalyst | Base | TON ² | Yield ³ |
|------------------|-------------------------------------|---------------------------------|------------------|------------------------|
| 1 | Fe ₃ O ₄ | NaOH | 0 | N. D. ⁴ |
| 2 ⁵ | Pd-Fe ₃ O ₄ | NaOH | 20 | 55 |
| 3 ⁶ | Au-Fe ₃ O ₄ | NaOH | 9 | 25 |
| 4 | AuPd-Fe ₃ O ₄ | NaOH | 23 | 65 |
| 5 | AuPd-Fe ₃ O ₄ | - | 5 | 14 |
| 6 ⁷ | AuPd-Fe ₃ O ₄ | NaOH | 15 | 43 |
| 7 | AuPd-Fe ₃ O ₄ | Cs ₂ CO ₃ | 25 | 69 |
| 8 | AuPd-Fe ₃ O ₄ | CsOH·H ₂ O | 33 | 90 ⁸ |
| 9 ⁹ | AuPd-Fe ₃ O ₄ | CsOH·H ₂ O | 33 | 92 (84 ¹⁰) |
| 10 ¹¹ | AuPd-Fe ₃ O ₄ | CsOH·H ₂ O | 32 | 89 |
| 11 ¹² | AuPd-Fe ₃ O ₄ | CsOH·H ₂ O | 15 | 42 ¹³ |
| 12 ¹⁴ | AuPd-Fe ₃ O ₄ | CsOH·H ₂ O | 89 | 71 |

¹ Reaction conditions: **1a** (0.20 mmol), catalyst (1.4 mol%), base (3.0 equiv), O₂ (1.0 atm), methanol (1.0 mL), r. t., 18 h. ² Turnover number (TON) = mmol of product/mmol of total metal except Fe. ³ Determined from ¹H NMR spectral analysis through the use of mesitylene as an internal standard. ⁴ N. D. = not detected. ⁵ Pd-Fe₃O₄ (2.8 mol%) was used as a catalyst. ⁶ Au-Fe₃O₄ (2.8 mol%) was used as a catalyst. ⁷ An air balloon was used instead of O₂. ⁸ An average value of three runs (91%, 90%, and 88%). ⁹ Result with **1a** (0.50 mmol) in MeOH (2.0 mL). ¹⁰ Yield of isolated product. ¹¹ Result with **1a** (1.0 mmol) in MeOH (1.0 mL), 4 h. ¹² Ethanol (1.0 mL) was used instead of methanol. ¹³ Yield of **2a'**. ¹⁴ Result with 0.40 mol% of catalyst.

Table 2. Base screening of the *N*-formylation of amine ¹.


| Entry | Base | Yield ² | Entry | Base | Yield ² |
|-------|-----------------------|--------------------|-------|---------------------------------|--------------------|
| 1 | - | 14 | 6 | K ₂ CO ₃ | 54 |
| 2 | LiOH·H ₂ O | 60 | 7 | Cs ₂ CO ₃ | 69 |
| 3 | NaOH | 65 | 8 | KOt Bu | 69 |
| 4 | KOH | 75 | 9 | K ₃ PO ₄ | 60 |
| 5 | CsOH·H ₂ O | 91 | 10 | CsF | 39 |

¹ Reaction conditions: **1a** (0.20 mmol), AuPd-Fe₃O₄ (1.4 mol%), base (3.0 equiv), O₂ (1.0 atm), methanol (1.0 mL), r. t., 18 h. ² Determined from ¹H NMR spectral analysis through the use of mesitylene as an internal standard.

3.3. Effect of Alloy Bimetallic Catalyst vs. Combination of Two Metal Catalysts

To investigate the distinctive advantage of the bimetallic nanocatalyst, several control experiments were conducted (Table 3). Because we used 1.4 mol% of AuPd-Fe₃O₄ to obtain the optimum results with **1a**, reactions with 2.8 mol% of either Au-Fe₃O₄ (entry 1) or Pd-Fe₃O₄ (entry 2) were performed under the standard reaction conditions to test the reactivity of each monometallic catalyst. The *N*-formylation reactions of *N*-methyl-1-phenylmethanamine, employing either Au or Pd catalysts, were not as efficient as that employing the AuPd catalyst (entry 4), giving 51% and 57% yields of **2a**, respectively. To further investigate the alloy nanocatalyst, we examined the reactions of other substrates, such as *N*-methyl-1-(*p*-tolyl)methanamine, 1-(4-methoxyphenyl)-*N*-methylmethanamine, *N*-methyl-1-(3-nitrophenyl)methanamine, and 3-(methylaminomethyl)benzotrile. With 2.8 mol% of Au-Fe₃O₄ (entry 1) or 2.8 mol% of Pd-Fe₃O₄ (entry 2), the reactions of secondary amines showed lower yields than those using AuPd-Fe₃O₄ (entry 4). These results indicate that both Au and Pd within the alloy catalyst contribute to product formation

through a synergistic effect [82–86]. When we used 1.4 mol% each of both Au–Fe₃O₄ and Pd–Fe₃O₄, interestingly the reaction of *N*-methyl-1-phenylmethanamine afforded 90% yield of the desired product (entry 3). The fact that similar product yields were obtained from the reactions employing AuPd and the combination of the Au and Pd toward *N*-methyl-1-phenylmethanamine was an exception rather than a general trend, as can be seen in the reactions of various substituted *N*-methylarylmethanamines. Reactions of other substrates with both Au–Fe₃O₄ and Pd–Fe₃O₄ provided the corresponding products with much lower yields than those obtained with the bimetallic AuPd catalyst. To rule out the possibility of homogeneous catalysis with both Au and Pd leached out into the solution, we carried out a filtration experiment [59,60]. The solution from a reaction of *N*-methyl-1-phenylmethanamine with 1.4 mol% AuPd–Fe₃O₄ under the optimized condition after 0.5 h was filtered through a syringe filter. The filtrated solution was then stirred for 6 h under O₂ atmosphere, and the progress of the reaction was checked. There was no further increase in the reaction yield. This result shows that the homogeneous solution did not drive the reaction further without the nanocatalyst, indicating that there is no catalysis from any homogeneous metal species. Next, we also tested the kinetics in the reaction of *N*-methyl-1-phenylmethanamine, employing either Au, Pd, a mixture of Au and Pd, or AuPd catalyst (Figure S14). The differences in the reaction rates indicate that there is a distinctive synergistic effect within the bimetallic catalyst, as the reaction employing this catalyst proceeded the fastest. Thus, considering both the product yields and the initial kinetics, there is an advantage in employing the bimetallic alloy catalyst, instead of using the monometallic catalysts separately.

Table 3. Comparison on the Effect of Alloy Bimetallic Catalyst and Combination of Two Metal Catalysts ¹.

Reaction scheme: $\text{R-C}_6\text{H}_4\text{-CH}_2\text{-NH-CH}_3$ (1, 0.20 mmol) $\xrightarrow[\text{MeOH, r. t., 18 h}]{\text{Catalyst, CsOH}\cdot\text{H}_2\text{O (3.0 equiv), O}_2 \text{ (1.0 atm)}}$ $\text{R-C}_6\text{H}_4\text{-CH}_2\text{-N(CH}_3\text{)-CHO}$ (2)

| Entry | Catalyst ³ | Product Yield with Various R Group (%) ² | | | | |
|----------------|-----------------------|---|------|-------|-------------------|------|
| | | H | 4-Me | 4-OMe | 3-NO ₂ | 3-CN |
| 1 ⁴ | Au | 51 | 61 | 27 | 25 | 23 |
| 2 ⁵ | Pd | 57 | 28 | 18 | 8 | 5 |
| 3 ⁶ | Au + Pd | 90 | 62 | 34 | 26 | 32 |
| 4 ⁷ | AuPd | 91 | 69 | 83 | 73 | 59 |

¹ Reaction conditions: **1** (0.20 mmol), catalyst, CsOH·H₂O (3.0 equiv), O₂ (1.0 atm), methanol (1.0 mL), r. t., 18 h. ² Yields were determined from ¹H NMR spectral analysis through the use of mesitylene as an internal standard. ³ Catalyst composition: Au–Fe₃O₄ (5.47 wt% Au), Pd–Fe₃O₄ (8.20 wt% Pd), AuPd–Fe₃O₄ (11.7 wt% Au, 6.23 wt% Pd, Au:Pd = 1:0.99). ⁴ Au–Fe₃O₄ (2.8 mol%) used. ⁵ Pd–Fe₃O₄ (2.8 mol%) used. ⁶ Au–Fe₃O₄ (1.4 mol%), Pd–Fe₃O₄ (1.4 mol%) used. ⁷ AuPd–Fe₃O₄ (1.4 mol%) used.

3.4. Substrate Scope

Using the optimized condition, we tested the *N*-formylation of various secondary amines bearing substituted aromatic rings, using 0.25 M of substrate over 18 h (Scheme 4). From the reaction of unsubstituted *N*-methyl-1-phenylmethanamine, *N*-formylated product was obtained in 84% (**2a**). Substrates bearing a methyl group on the aromatic ring furnished a good product yield, regardless of its position (**2b–2d**). Reactivity was maintained in the case of a substrate with two methyl groups on the aromatic ring (**2e**). High yield (87%) was also observed from a sterically hindered substrate possessing methyl groups at positions 2 and 6 (**2f**) when the reaction was run at 0.20 M (0.20 mmol scale). The reactions of substrates possessing a strong electron-donating methoxy group resulted in good yields (81% and 83%, **2g** and **2h**, respectively). The reaction of *N*-methyl-1-(naphthalen-1-yl)methanamine also resulted in good yield (80%, **2i**). When an electron-withdrawing group exists on the aromatic ring, good to moderate yields of the desired products were obtained (85%, 83%,

61% and 58% for **2l**–**2o**, respectively). Reactions of substrates bearing fluorine(s) resulted in acceptable product yields (73% and 79% for **2j** and **2k**, respectively). Interestingly, reactions of amines with trifluoromethyl groups at the 3 or 4 position on the aromatic ring furnished good yields (85%, 83%, and 75% for **2l**, **2m**, and **2q**, respectively) compared with other electron-deficient amines. Reactions of substrates possessing other electron-withdrawing substituents, such as nitro- or cyano- groups, yielded products with 61% and 58% yields (**2n** and **2o**), respectively. In addition, the reaction of *N*-methylaniline resulted in the desired formylated product in 82% yield (**2p**). We confirmed that not only *N*-methylamines, but other *N*-alkyl-substituted secondary amines are also good substrates for the reaction, as shown in the case of **2q** and **2r**, with the reaction of *N,N*-dibenzylamine, resulting in 73% yield (**2r**). In the reactions of non-benzylic secondary alkylamines, products were obtained in moderate yields (55%, 57%, and 66%, **2s**–**2u**, respectively). We hypothesized that the reactions could be run at higher concentrations and thus expedited. When reactions were conducted at 1.0 M, most were completed in 6–8 h instead of 18 h at 0.20 M. The reactions of several substrates maintained their yields at higher concentrations in shorter reaction times, and the results are shown in the supporting information (Table S6).

3.5. Mechanistic Investigation

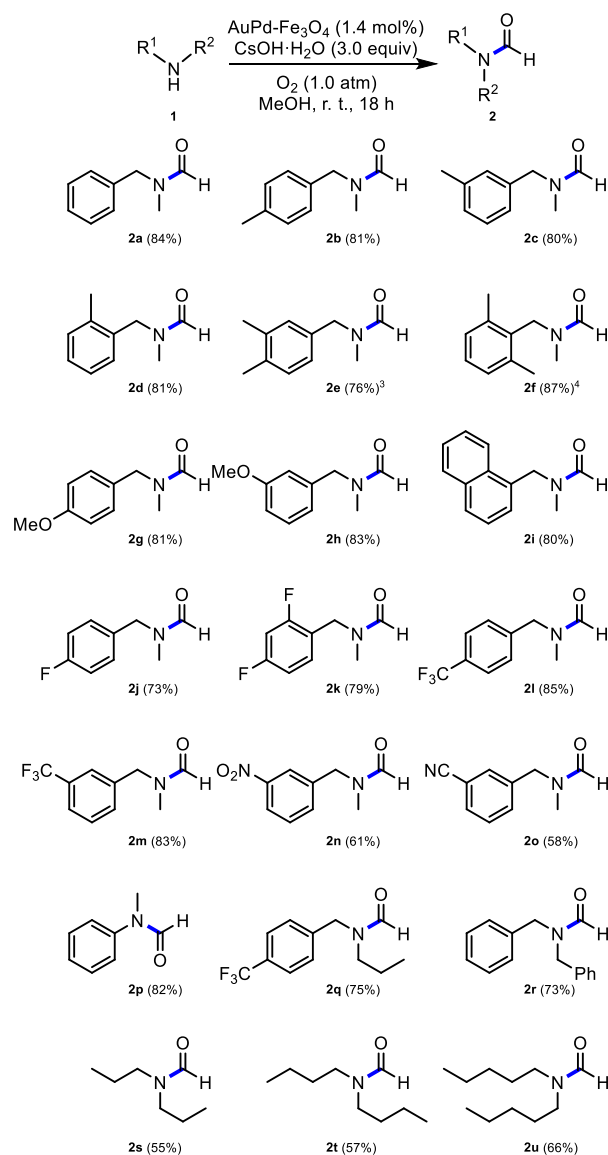
Based on the results of optimization and the substrate scope investigation, we conducted several kinetic experiments and control experiments to probe the reaction mechanism (Figures S15 and S16, and Table S7). To summarize the results, the amine substrate (**1**) is consumed under oxidative condition in the presence of AuPd–Fe₃O₄ catalyst in methanol. The oxidation of methanol in the presence of the catalyst by the assistance of a base generates mostly HCHO and a small portion of HCO₂Me, which rapidly react with an amine to furnish *N*-formamide (**2**). The formation of HCO₂H from methanol was ruled out because almost no HCO₂H was detected from the control oxidation of methanol. Both methanol and the resulting hemiaminal intermediate (**3**) are oxidized by the AuPd–Fe₃O₄ catalyst. These results are presented in Scheme 5.

3.6. Effect of Au:Pd Ratio and Various Supports

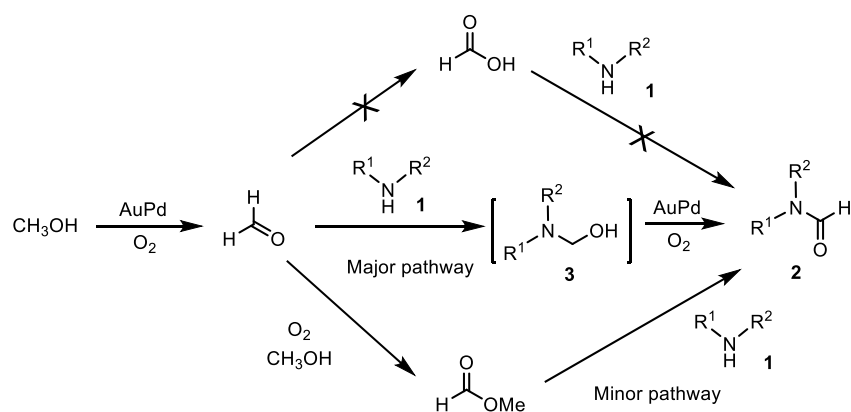
To further investigate the correlation between the Au:Pd ratio and the product yield, we synthesized catalysts with various Au:Pd ratios and tested them using 2.0 mol% of catalyst under the same reaction condition (Table 4 and Figure S10). The ~1:1 atomic ratio of Au and Pd was found to be the best combination. Additionally, to test the effect of iron oxide, we synthesized several AuPd catalysts with various supports for comparison (Tables S4 and S5 and Figure S13). AuPd on the iron oxide support showed the highest reactivity for *N*-formylation.

3.7. Recycling Test

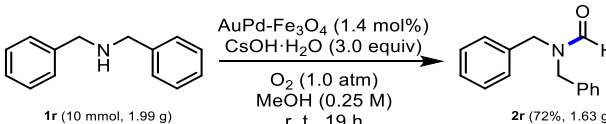
Because heterogeneous catalysts are employed for easy recovery and reuse, the recyclability of AuPd–Fe₃O₄ was tested based on the optimized condition (Figure 3). In the recycling experiment with **1a**, the catalytic activity was maintained without significant loss of yield. Based on our previous report [66], a strong base disintegrates the iron oxide support, resulting in poor recyclability. However, the catalytic activity was somehow maintained for 9 cycles. When the SEM and HR-TEM images of the catalyst after 10 cycles were examined, Au and Pd particles appeared to be significantly agglomerated (Figures S11 and S12). Additionally, the ICP-AES data of the used catalyst showed lower Au and Pd contents (wt%) (Figure S8). Therefore, considering the excess amount of strong base and oxidative environment that can be detrimental to the catalyst, our reaction system has some reusability advantages.



Scheme 4. Substrate scope of *N*-formylation^{1,2,1} Isolated yield. ² **1** (0.50 mmol), $\text{AuPd-Fe}_3\text{O}_4$ (1.4 mol%), $\text{CsOH}\cdot\text{H}_2\text{O}$ (3.0 equiv), O_2 (1.0 atm), methanol (2.0 mL), r. t., 18 h. ³ 2.4 mol% of $\text{AuPd-Fe}_3\text{O}_4$ used. ⁴ The reaction was run at 0.20 mmol scale of **1f** in methanol (1.0 mL).

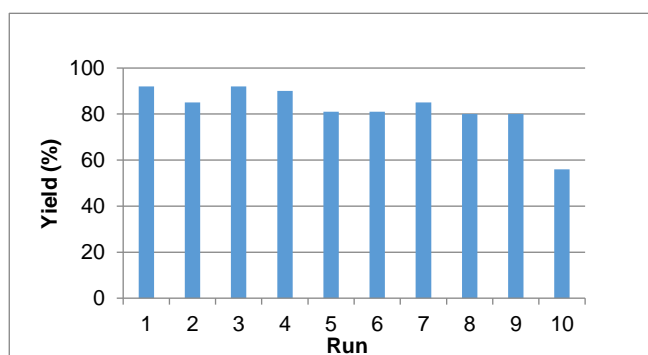


Scheme 5. A plausible reaction pathway for *N*-formylation of amines.

Table 4. Reactivity comparison of various AuPd catalysts ¹.


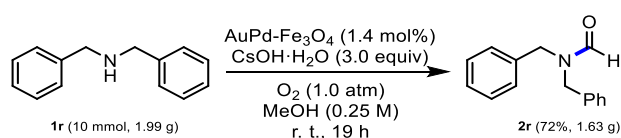
| Entry | Catalyst | Yield ² |
|-------|--|--------------------|
| 1 | Au ₁ Pd _{0.23} -Fe ₃ O ₄ | 76 |
| 2 | Au ₁ Pd _{0.39} -Fe ₃ O ₄ | 76 |
| 3 | Au ₁ Pd _{1.08} -Fe ₃ O ₄ | 91 |
| 4 | Au _{0.65} Pd ₁ -Fe ₃ O ₄ | 79 |
| 5 | Au _{0.39} Pd ₁ -Fe ₃ O ₄ | 69 |

¹ Reaction conditions: **1a** (0.20 mmol), catalyst (2.0 mol%), CsOH·H₂O (3.0 equiv), O₂ (1.0 atm), methanol (1.0 mL), r. t., 18 h. ² Determined from ¹H NMR spectral analysis through the use of mesitylene as an internal standard.

**Figure 3.** Results of recycling test.

3.8. Gram Scale Reaction

We subsequently performed a gram-scale reaction (Scheme 6). At a 10 mmol scale, the reaction of **1r** afforded **2r** in 72% yield, demonstrating the viability of the reaction in organic synthesis.

**Scheme 6.** Gram scale reaction.

4. Conclusions

In conclusion, we developed a novel catalytic system for the mild synthesis of formamides in good-to-moderate yields. Utilizing a reusable AuPd bimetallic nanocatalyst, we synthesized formamides at room temperature under atmospheric pressure of O₂. The use of methanol as the formyl source, instead of toxic or polluting reagents, bodes well for sustainable organic synthesis. During the investigation of various catalysts, the bimetallic alloy AuPd-Fe₃O₄ catalyst proved to be superior to either of the monometallic catalysts. Based on the product yield and initial kinetics, there appears to be a synergistic effect between the Au and Pd during the reaction. The broad substrate scope could enlarge the *N*-formylation reaction library. The formamide yield was the highest when the Au: Pd ratio was ~1:1. In addition, the AuPd on the Fe₃O₄ support proved to be more effective than AuPd catalysts on other supports. Furthermore, the reaction was scalable to the gram scale. This new method avoids the requirements of high temperature and high pressure of O₂ gas. Moreover, the good recyclability of the catalyst broadens the potential applications of the reaction.

Supplementary Materials: The following are available online at <https://www.mdpi.com/article/10.3390/nano11082101/s1>, Table S1: Catalyst screening, Table S2. Base screening, Table S3. Catalyst loading, Figure S1. SEM analysis, Figure S2. SEM-EDS analysis, Figure S3. EDS map spectrum, Figure S4. HR-TEM analysis, Figure S5. BF-STEM and HAADF-STEM analysis, Figure S6. Particle distribution of AuPd-NPs, Figure S7. XPS analysis, Figure S8. ICP-AES analysis, Figure S9. XRD analysis, Figure S10. SEM, EDS, and ICP-AES analysis of Au_xPd_y-Fe₃O₄, Figure S11. SEM analysis of recycled catalyst, Figure S12. HR-TEM analysis of recycled catalyst, Figure S13. SEM analysis of other AuPd-NPs, Table S4. ICP-AES of other AuPd-NPs, Table S5. Formylation data with other AuPd-NPs, Figure S14. Kinetic data of *N*-formylation, Table S6. Substrate scope under high substrate concentration, Figure S15. Determination of the methanol oxidation products, Figure S16. Initial kinetics of HCHO-DNPH generation, Table S7. Control experiments.

Author Contributions: Conceptualization, experimental methodology, catalytic study, and manuscript writing, S.Y.; products analysis, S.Y., A.C. and J.H.C.; supervision of the project and manuscript editing, B.M.K. All authors have read and agreed to the published version of the manuscript.

Funding: B.M.K. thanks the Nano Material Development Program (NRF-2012-M3A7B4049644) and the Mid-Career Researcher Program (NRF-2019-R1A2C1004173) for an NRF grant funded by MEST.

Data Availability Statement: Data are contained within the article or Supplementary Materials.

Conflicts of Interest: The authors declare no conflict of interest.

References

1. Gerack, C.J.; McElwee-White, L. Formylation of Amines. *Molecules* **2014**, *19*, 7689–7713. [CrossRef]
2. Schardl, C.L.; Grossman, R.B.; Nagabhyru, P.; Faulkner, J.R.; Mallik, U.P. Loline alkaloids: Currencies of mutualism. *Phytochemistry* **2007**, *68*, 980–996. [CrossRef]
3. Thauer, R.K. Biochemistry of methanogenesis: A tribute to Marjory Stephenson. *Microbiology* **1998**, *144*, 2377–2406. [CrossRef]
4. Wada, T.; Takagi, H.; Minakami, H.; Hamanaka, W.; Okamoto, K.; Ito, A.; Sahashi, Y. A New Thiamine Derivative, S-Benzoylthiamine O-Monophosphate. *Science* **1961**, *134*, 195–196. [CrossRef] [PubMed]
5. Forsch, R.A.; Rosowsky, A. A New One-Step Synthesis of Leucovorin from Folic Acid and of 5-Formyl-5,6,7,8-tetrahydrohomofolic Acid from Homofolic Acid Using Dimethylamine-Borane in Formic Acid. *J. Org. Chem.* **1985**, *50*, 2582–2583. [CrossRef]
6. Ravina, E. *The Evolution of Drug Discovery: From Traditional Medicines to Modern Drugs*; Wiley-VCH: Weinheim, Germany, 2011; pp. 157–159.
7. Lonsdale, D. Thiamine tetrahydrofurfuryl disulfide: A little known therapeutic agent. *Med. Sci. Monit.* **2004**, *10*, RA199–RA203. [PubMed]
8. Olah, G.A.; Ohannesian, L.; Arvanaghi, M. Formylating Agents. *Chem. Rev.* **1987**, *87*, 671–686. [CrossRef]
9. Bao, K.; Zhang, W.; Bu, X.; Song, Z.; Zhang, L.; Cheng, M. A novel type of *N*-formylation and related reactions of amines via cyanides and esters as formylating agents. *Chem. Commun.* **2008**, *42*, 5429–5431. [CrossRef]
10. Ke, Z.; Zhang, Y.; Cui, X.; Shi, F. Supported nano-gold-catalyzed *N*-formylation of amines with paraformaldehyde in water under ambient conditions. *Green Chem.* **2016**, *18*, 808–816. [CrossRef]
11. Blicke, F.F.; Lu, C.-J. Formylation of Amines with Chloral and Reduction of the *N*-Formyl Derivatives with Lithium Aluminum Hydride. *J. Am. Chem. Soc.* **1952**, *74*, 3933–3934. [CrossRef]
12. Yale, H.L. Formylation of Amines with Phenyl Formate. *J. Org. Chem.* **1971**, *36*, 3238–3240. [CrossRef]
13. Djuric, S.W. A Mild and Convenient Procedure for the *N*-Formylation of Secondary Amines Using Organosilicon Chemistry. *J. Org. Chem.* **1984**, *49*, 1311–1312. [CrossRef]
14. Hosseini-Sarvari, M.; Sharghi, H. ZnO as a New Catalyst for *N*-Formylation of Amines under Solvent-Free Conditions. *J. Org. Chem.* **2006**, *71*, 6652–6654. [CrossRef] [PubMed]
15. Reddy, P.G.; Kumar, G.D.K.; Baskaran, S. A convenient method for the *N*-formylation of secondary amines and anilines using ammonium formate. *Tetrahedron Lett.* **2000**, *41*, 9149–9151. [CrossRef]
16. Bhojgowd, M.R.M.; Nizam, A.; Pasha, M.A. Amberlite IR-120: A Reusable Catalyst for *N*-Formylation of Amines with Formic Acid Using Microwaves. *Chin. J. Catal.* **2010**, *31*, 518–520. [CrossRef]
17. Wang, Z.-G.; Lu, M. Highly efficient *N*-formylation of amines with ammonium formate catalyzed by nano-Fe₃O₄ in PEG-400. *RSC Adv.* **2014**, *4*, 1234–1240. [CrossRef]
18. Keim, W. C₁ Chemistry: Potential and developments. *Pure Appl. Chem.* **1986**, *58*, 825–832. [CrossRef]
19. Natte, K.; Neumann, H.; Beller, M.; Jagadeesh, R.V. Transition-Metal-Catalyzed Utilization of Methanol as a C₁ Source in Organic Synthesis. *Angew. Chem. Int. Ed.* **2017**, *56*, 6384–6394. [CrossRef]
20. Grigg, R.; Mitchell, T.R.B.; Sutthivaiyakit, S.; Tongpenyai, N. Transition Metal-catalysed *N*-Alkylation of Amines by Alcohols. *J. Chem. Soc. Chem. Commun.* **1981**, *12*, 611–612. [CrossRef]

21. Dang, T.T.; Ramalingam, B.; Seayad, A.M. Efficient Ruthenium-Catalyzed N-Methylation of Amines Using Methanol. *ACS Catal.* **2015**, *5*, 4082–4088. [[CrossRef](#)]
22. Elangovan, S.; Neumann, J.; Sortais, J.-B.; Junge, K.; Darcel, C.; Beller, M. Efficient and selective N-alkylation of amines with alcohols catalysed by manganese pincer complexes. *Nat. Commun.* **2016**, *7*, 12641–12648. [[CrossRef](#)]
23. Chen, Y. Recent Advances in Methylation: A Guide for Selecting Methylation Reagents. *Chem. Eur. J.* **2019**, *25*, 3405–3439. [[CrossRef](#)]
24. Meng, C.; Liu, P.; Tung, N.T.; Han, X.; Li, F. N-Methylation of Amines with Methanol in Aqueous Solution Catalyzed by a Water-Soluble Metal–Ligand Bifunctional Dinuclear Iridium Catalyst. *J. Org. Chem.* **2020**, *85*, 5815–5824. [[CrossRef](#)]
25. Yu, H.; Wu, Z.; Wei, Z.; Zhai, Y.; Ru, S.; Zhao, Q.; Wang, J.; Han, S.; Wei, Y. N-formylation of amines using methanol as a potential formyl carrier by a reusable chromium catalyst. *Commun. Chem.* **2019**, *2*, 15–21. [[CrossRef](#)]
26. Nasrollahzadeh, M.; Motahharifar, N.; Sajjadi, M.; Aghbolagh, A.M.; Shokouhimehr, M.; Varma, R.S. Recent advances in N-formylation of amines and nitroarenes using efficient (nano)catalysts in ecofriendly media. *Green Chem.* **2019**, *21*, 5144–5167. [[CrossRef](#)]
27. Pichardo, M.C.; Tavakoli, G.; Armstrong, J.E.; Wilczek, T.; Thomas, B.E.; Prechtel, M.H.G. Copper-Catalyzed Formylation of Amines by using Methanol as the C1 Source. *ChemSusChem* **2020**, *13*, 882–887. [[CrossRef](#)] [[PubMed](#)]
28. Gowrisankar, S.; Neumann, H.; Beller, M. A Convenient and Practical Synthesis of Anisoles and Deuterated Anisoles by Palladium-Catalyzed Coupling Reactions of Aryl Bromides and Chlorides. *Chem. Eur. J.* **2012**, *18*, 2498–2502. [[CrossRef](#)]
29. Dash, P.; Janni, M.; Peruncheralathan, S. Trideuteriomethoxylation of Aryl and Heteroaryl Halides. *Eur. J. Org. Chem.* **2012**, *26*, 4914–4917. [[CrossRef](#)]
30. Baumann, M.; Baxendale, I.R. An overview of the synthetic routes to the best selling drugs containing 6-membered heterocycles. *Beilstein J. Org. Chem.* **2013**, *9*, 2265–2319. [[CrossRef](#)]
31. Cole-Hamilton, D.J. Homogeneous Catalysis—New Approaches to Catalyst Separation, Recovery, and Recycling. *Science* **2003**, *299*, 1702–1706. [[CrossRef](#)]
32. Hartwig, J.F.; Collman, J.P. *Organotransition Metal Chemistry: From Bonding to Catalysis*; University Science Books: Sausalito, CA, USA, 2010; pp. 546–549.
33. Crabtree, R.H. Resolving Heterogeneity Problems and Impurity Artifacts in Operationally Homogeneous Transition Metal Catalysts. *Chem. Rev.* **2012**, *112*, 1536–1554. [[CrossRef](#)] [[PubMed](#)]
34. Ortega, N.; Richter, C.; Glorius, F. N-Formylation of Amines by Methanol Activation. *Org. Lett.* **2013**, *15*, 1776–1779. [[CrossRef](#)]
35. Chakraborty, S.; Gellrich, U.; Diskin-Posner, Y.; Leitus, G.; Avram, L.; Milstein, D. Manganese-Catalyzed N-Formylation of Amines by Methanol Liberating H₂: A Catalytic and Mechanistic Study. *Angew. Chem. Int. Ed.* **2017**, *56*, 4229–4233. [[CrossRef](#)]
36. Kang, B.; Hong, S.H. Hydrogen Acceptor- and Base-Free N-Formylation of Nitriles and Amines using Methanol as C₁ Source. *Adv. Synth. Catal.* **2015**, *357*, 834–840. [[CrossRef](#)]
37. Choi, G.; Hong, S.H. Selective N-Formylation and N-Methylation of Amines Using Methanol as a Sustainable C₁ Source. *ACS Sustain. Chem. Eng.* **2019**, *7*, 716–723. [[CrossRef](#)]
38. Shekhar, A.C.; Kumar, A.R.; Sathaiyah, G.; Paul, V.L.; Sridhar, M.; Rao, P.S. Facile N-formylation of amines using Lewis acids as novel catalysts. *Tetrahedron Lett.* **2009**, *50*, 7099–7101. [[CrossRef](#)]
39. Pathare, S.P.; Sawant, R.V.; Akamanchi, K.G. Sulfated tungstate catalyzed highly accelerated N-formylation. *Tetrahedron Lett.* **2012**, *53*, 3259–3263. [[CrossRef](#)]
40. Khojastehnezhad, A.; Rahimizadeh, M.; Moeinpour, F.; Eshghi, H.; Bakavoli, M. Polyphosphoric acid supported on silica-coated NiFe₂O₄ nanoparticles: An efficient and magnetically-recoverable catalyst for N-formylation of amines. *C. R. Chim.* **2014**, *17*, 459–464. [[CrossRef](#)]
41. Kooti, M.; Nasiri, E. Phosphotungstic acid supported on silica-coated CoFe₂O₄ nanoparticles: An efficient and magnetically-recoverable catalyst for N-formylation of amines under solvent-free conditions. *J. Mol. Catal. A Chem.* **2015**, *406*, 168–177. [[CrossRef](#)]
42. Baig, R.B.N.; Verma, S.; Nadagouda, M.N.; Varma, R.S. A photoactive bimetallic framework for direct aminoforylation of nitroarenes. *Green Chem.* **2016**, *18*, 1019–1022. [[CrossRef](#)]
43. Luo, R.; Lin, X.; Chen, Y.; Zhang, W.; Zhou, X.; Ji, H. Cooperative Catalytic Activation of Si–H Bonds: CO₂-Based Synthesis of Formamides from Amines and Hydrosilanes under Mild Conditions. *ChemSusChem* **2017**, *10*, 1224–1232. [[CrossRef](#)]
44. Huang, Z.; Jiang, X.; Zhou, S.; Yang, P.; Du, C.-X.; Li, Y. Mn-Catalyzed Selective Double and Mono-N-Formylation and N-Methylation of Amines by using CO₂. *ChemSusChem* **2019**, *12*, 3054–3059. [[CrossRef](#)]
45. Polshettiwar, V.; Varma, R.S. Green chemistry by nano-catalysis. *Green Chem.* **2010**, *12*, 743–754. [[CrossRef](#)]
46. Polshettiwar, V.; Luque, R.; Fihri, A.; Zhu, H.; Bouhrara, M.; Basset, J.-M. Magnetically Recoverable Nanocatalysts. *Chem. Rev.* **2011**, *111*, 3036–3075. [[CrossRef](#)]
47. Gawande, M.B.; Branco, P.S.; Varma, R.S. Nano-magnetite (Fe₃O₄) as a support for recyclable catalysts in the development of sustainable methodologies. *Chem. Soc. Rev.* **2013**, *42*, 3371–3393. [[CrossRef](#)]
48. Enache, D.I.; Edwards, J.K.; Landon, P.; Solsona-Espriu, B.; Carley, A.F.; Herzing, A.A.; Watanabe, M.; Kiely, C.J.; Knight, D.W.; Hutchings, G.J. Solvent-Free Oxidation of Primary Alcohols to Aldehydes Using Au-Pd/TiO₂ Catalysts. *Science* **2006**, *311*, 362–365. [[CrossRef](#)]

49. Hou, W.; Dehm, N.A.; Scott, R.W.J. Alcohol oxidations in aqueous solutions using Au, Pd, and bimetallic AuPd nanoparticle catalysts. *J. Catal.* **2008**, *253*, 22–27. [[CrossRef](#)]
50. Chang, C.-R.; Long, B.; Yang, X.-F.; Li, J. Theoretical Studies on the Synergetic Effects of Au–Pd Bimetallic Catalysts in the Selective Oxidation of Methanol. *J. Phys. Chem. C* **2015**, *119*, 16072–16081. [[CrossRef](#)]
51. Han, S.; Mullins, C.B. Surface Alloy Composition Controlled O₂ Activation on Pd–Au Bimetallic Model Catalysts. *ACS Catal.* **2018**, *8*, 3641–3649. [[CrossRef](#)]
52. Preedasuriyachai, P.; Kitahara, H.; Chavasiri, W.; Sakurai, H. N-Formylation of Amines Catalyzed by Nanogold under Aerobic Oxidation Conditions with MeOH or Formalin. *Chem. Lett.* **2010**, *39*, 1174–1176. [[CrossRef](#)]
53. Ishida, T.; Haruta, M. N-Formylation of Amines via the Aerobic Oxidation of Methanol over Supported Gold Nanoparticles. *ChemSusChem* **2009**, *2*, 538–541. [[CrossRef](#)]
54. Tumma, H.; Nagaraju, N.; Reddy, K.V. A facile method for the N-formylation of primary and secondary amines by liquid phase oxidation of methanol in the presence of hydrogen peroxide over basic copper hydroxyl salts. *J. Mol. Catal. A* **2009**, *310*, 121–129. [[CrossRef](#)]
55. Tanaka, S.; Minato, T.; Ito, E.; Hara, M.; Kim, Y.; Yamamoto, Y.; Asao, N. Selective Aerobic Oxidation of Methanol in the Coexistence of Amines by Nanoporous Gold Catalysts: Highly Efficient Synthesis of Formamides. *Chem. Eur. J.* **2013**, *19*, 11832–11836. [[CrossRef](#)]
56. Jang, Y.; Chung, J.; Kim, S.; Jun, S.W.; Kim, B.H.; Lee, D.W.; Kim, B.M.; Hyeon, T. Simple synthesis of Pd–Fe₃O₄ heterodimer nanocrystals and their application as a magnetically recyclable catalyst for Suzuki cross-coupling reactions. *Phys. Chem. Chem. Phys.* **2011**, *13*, 2512–2516. [[CrossRef](#)]
57. Jang, Y.; Kim, S.; Jun, S.W.; Kim, B.H.; Hwang, S.; Song, I.K.; Kim, B.M.; Hyeon, T. Simple one-pot synthesis of Rh–Fe₃O₄ heterodimer nanocrystals and their applications to a magnetically recyclable catalyst for efficient and selective reduction of nitroarenes and alkenes. *Chem. Commun.* **2011**, *47*, 3601–3603. [[CrossRef](#)]
58. Lee, J.; Chung, J.; Byun, S.; Kim, B.M.; Lee, C. Direct catalytic C–H arylation of imidazo [1,2-a]pyridine with aryl bromides using magnetically recyclable Pd–Fe₃O₄ nanoparticles. *Tetrahedron* **2013**, *69*, 5660–5664. [[CrossRef](#)]
59. Chung, J.; Kim, J.; Jang, Y.; Byun, S.; Hyeon, T.; Kim, B.M. Heck and Sonogashira cross-coupling reactions using recyclable Pd–Fe₃O₄ heterodimeric nanocrystal catalysts. *Tetrahedron Lett.* **2013**, *54*, 5192–5196. [[CrossRef](#)]
60. Byun, S.; Chung, J.; Jang, Y.; Kwon, J.; Hyeon, T.; Kim, B.M. Highly selective Wacker oxidation of terminal olefins using magnetically recyclable Pd–Fe₃O₄ heterodimer nanocrystals. *RSC Adv.* **2013**, *3*, 16296–16299. [[CrossRef](#)]
61. Bae, I.H.; Lee, I.-H.; Byun, S.; Chung, J.; Kim, B.M.; Choi, T.-L. Magnetically Recyclable Pd–Fe₃O₄ Heterodimer Nanocrystals for the Synthesis of Conjugated Polymers via Suzuki Polycondensation: Toward Green Chemistry. *J. Polym. Sci. Pol. Chem.* **2014**, *52*, 1525–1528. [[CrossRef](#)]
62. Kwon, J.; Chung, J.; Byun, S.; Kim, B.M. Efficient Synthesis of Indole Derivatives via Tandem Cyclization Catalyzed by Magnetically Recoverable Palladium/Magnetite (Pd–Fe₃O₄) Nanocrystals. *Asian J. Org. Chem.* **2016**, *5*, 470–476. [[CrossRef](#)]
63. Byun, S.; Song, Y.; Kim, B.M. Heterogenized Bimetallic Pd–Pt–Fe₃O₄ Nanoflakes as Extremely Robust, Magnetically Recyclable Catalysts for Chemoselective Nitroarene Reduction. *ACS Appl. Mater. Interfaces* **2016**, *8*, 14637–14647. [[CrossRef](#)]
64. Jang, J.; Byun, S.; Kim, B.M.; Lee, S. Arylsilylation of aryl halides using the magnetically recyclable bimetallic Pd–Pt–Fe₃O₄ catalyst. *Chem. Commun.* **2018**, *54*, 3492–3495. [[CrossRef](#)]
65. Cho, A.; Byun, S.; Kim, B.M. AuPd–Fe₃O₄ Nanoparticle Catalysts for Highly Selective, One-Pot Cascade Nitro-Reduction and Reductive Amination. *Adv. Synth. Catal.* **2018**, *360*, 1253–1261. [[CrossRef](#)]
66. Cho, A.; Byun, S.; Cho, J.H.; Kim, B.M. AuPd–Fe₃O₄ Nanoparticle-Catalyzed Synthesis of Furan-2,5-dimethylcarboxylate from 5-Hydroxymethylfurfural under Mild Conditions. *ChemSusChem* **2019**, *12*, 2310–2317. [[CrossRef](#)]
67. Cho, J.H.; Byun, S.; Cho, A.; Kim, B.M. One-pot, chemoselective synthesis of secondary amines from aryl nitriles using a PdPt–Fe₃O₄ nanoparticle catalyst. *Catal. Sci. Technol.* **2020**, *10*, 4201–4209. [[CrossRef](#)]
68. Wang, R.; Wu, Z.; Chen, C.; Qin, Z.; Zhu, H.; Wang, G.; Wang, H.; Wu, C.; Dong, W.; Fan, W.; et al. Graphene-supported Au–Pd bimetallic nanoparticles with excellent catalytic performance in selective oxidation of methanol to methyl formate. *Chem. Commun.* **2013**, *49*, 8250–8252. [[CrossRef](#)]
69. Zhu, X.; Guo, Q.; Sun, Y.; Chen, S.; Wang, J.-Q.; Wu, M.; Fu, W.; Tang, Y.; Duan, X.; Chen, D.; et al. Optimising surface d charge of AuPd nanoalloy catalysts for enhanced catalytic activity. *Nat. Commun.* **2019**, *10*, 1428–1438. [[CrossRef](#)]
70. Ju, P.; Chen, J.; Chen, A.; Chen, L.; Yu, Y. N-Formylation of Amines with CO₂ and H₂ Using Pd–Au Bimetallic Catalysts Supported on Polyaniline-Functionalized Carbon Nanotubes. *ACS Sustain. Chem. Eng.* **2017**, *5*, 2516–2528.
71. Wang, R.; Wu, Z.; Wang, G.; Qin, Z.; Chen, C.; Dong, M.; Zhu, H.; Fan, W.; Wang, J. Highly active Au–Pd nanoparticles supported on three-dimensional graphene–carbon nanotube hybrid for selective oxidation of methanol to methyl formate. *RSC Adv.* **2015**, *5*, 44835–44839. [[CrossRef](#)]
72. Beller, M. The Current Status and Future Trends in Oxidation Chemistry. *Adv. Synth. Catal.* **2004**, *346*, 107–108. [[CrossRef](#)]
73. Harit, H.; Hiran, B.L.; Joshi, S.N. Kinetics and Mechanism of Oxidation of Primary Alcohols by Pyridinium Dichromate. *Chem. Sci. Trans.* **2015**, *4*, 49–58.
74. Jana, S.; Thomas, J.; Gupta, S.S. Catalytic oxidation of alcohols using Fe-bTAML and NaClO: Comparing the reactivity of Fe(V)O and Fe(IV)O intermediates. *Inorg. Chim. Acta* **2019**, *486*, 476–482. [[CrossRef](#)]
75. Mallat, T.; Baiker, A. Oxidation of Alcohols with Molecular Oxygen on Solid Catalysts. *Chem. Rev.* **2004**, *104*, 3037–3058. [[CrossRef](#)]

76. Punniyamurthy, T.; Velusamy, S.; Iqbal, J. Recent Advances in Transition Metal Catalyzed Oxidation of Organic Substrates with Molecular Oxygen. *Chem. Rev.* **2005**, *105*, 2329–2363. [[CrossRef](#)]
77. Camellone, M.F.; Marx, D. Nature and Role of Activated Molecular Oxygen Species at the Gold/Titania Interface in the Selective Oxidation of Alcohols. *J. Phys. Chem. C* **2014**, *118*, 20989–21000. [[CrossRef](#)]
78. Whiting, G.T.; Kondrat, S.A.; Hammond, C.; Dimitratos, N.; He, Q.; Morgan, D.J.; Dummer, N.F.; Bartley, J.K.; Kiely, C.J.; Taylor, S.H.; et al. Methyl Formate Formation from Methanol Oxidation Using Supported Gold–Palladium Nanoparticles. *ACS Catal.* **2015**, *5*, 637–644. [[CrossRef](#)]
79. Tong, X.; Liu, Z.; Yu, L.; Li, Y. A tunable process: Catalytic transformation of renewable furfural with aliphatic alcohols in the presence of molecular oxygen. *Chem. Commun.* **2015**, *51*, 3674–3677. [[CrossRef](#)]
80. Slot, T.K.; Eisenberg, D.; van Noordenne, D.; Jungbacker, P.; Rothenberg, G. Cooperative Catalysis for Selective Alcohol Oxidation with Molecular Oxygen. *Chem. Eur. J.* **2016**, *22*, 12307–12311. [[CrossRef](#)]
81. Ray, R.; Chandra, S.; Maiti, D.; Lahiri, G.K. Simple and Efficient Ruthenium-Catalyzed Oxidation of Primary Alcohols with Molecular Oxygen. *Chem. Eur. J.* **2016**, *22*, 8814–8822. [[CrossRef](#)]
82. Jiang, H.-L.; Xu, Q. Recent progress in synergistic catalysis over heterometallic nanoparticles. *J. Mater. Chem.* **2011**, *21*, 13705–13725. [[CrossRef](#)]
83. Singh, A.K.; Xu, Q. Synergistic Catalysis over Bimetallic Alloy Nanoparticles. *ChemCatChem* **2013**, *5*, 652–676. [[CrossRef](#)]
84. Wang, S.; Zhang, D.; Ma, Y.; Zhang, H.; Gao, J.; Nie, Y.; Sun, X. Aqueous Solution Synthesis of Pt–M (M = Fe, Co, Ni) Bimetallic Nanoparticles and Their Catalysis for the Hydrolytic Dehydrogenation of Ammonia Borane. *ACS Appl. Mater. Interfaces* **2014**, *6*, 12429–12435. [[CrossRef](#)]
85. Yu, H.; Tang, W.; Li, K.; Zhao, S.; Yin, H.; Zhou, S. Enhanced Catalytic Performance for Hydrogenation of Substituted Nitroaromatics over Ir-Based Bimetallic Nanocatalysts. *ACS Appl. Mater. Interfaces* **2019**, *11*, 6958–6969. [[CrossRef](#)]
86. Wang, M.; Chen, D.; Li, N.; Xu, Q.; Li, H.; He, J.; Lu, J. Highly Efficient Catalysts of Bimetallic Pt–Ru Nanocrystals Supported on Ordered ZrO₂ Nanotube for Toluene Oxidation. *ACS Appl. Mater. Interfaces* **2020**, *12*, 13781–13789. [[CrossRef](#)]